Acta Polytechnica **64**(5):430–436, 2024
https://doi.org/10.14311/AP.2024.64.0430

Published by the Czech Technical University in Prague

DRECE METHOD FOR CONTINUOUS SEVERE PLASTIC DEFORMATION OF CUZN37 SHEETS

Martin Pastrňák[a,*], Radek Čada[a], Tomáš Pektor[a], Stanislav Rusz[a], František Tatíček[b], Jarosław Mizera[c], Marie Pastrňáková[d]

[a] *Technical University of Ostrava, Faculty of Mechanical Engineering, Department of Mechanical Technology, 17. listopadu 15, 708 00 Ostrava, Czech Republic*

[b] *Czech Technical University in Prague, Faculty of Mechanical Engineering, Department of Manufacturing Technology, Technická 4, 166 07 Prague, Czech Republic*

[c] *Warsaw University of Technology, Faculty of Materials Science and Engineering, Division of Materials Design, Wołoska 141, 02-507 Warsaw, Poland*

[d] *Technical University of Ostrava, Faculty of Mining and Geology, Department of Environmental Engineering, 17. listopadu 15, 708 00 Ostrava, Czech Republic*

[*] corresponding author: martin.pastrnak@vsb.cz

Abstract. This paper presents a continuous severe plastic deformation (SPD) process for sheet metal called Dual Rolls Equal Channel Extrusion (DRECE) is introduced. The DRECE process achieves maximum sheet metal deformation by combining bending deformation with channel-angular shear deformation. The evolution of the microstructure and mechanical properties of the CuZn37 alloy has been experimentally investigated as a function of the number of repeated DRECE passes. The DRECE process was repeated up to four times at room temperature. As the number of passes increased, the character of the microstructure was gradually strongly deformed by intensive shear deformation. The microhardness and tensile properties changed significantly as a function of the number of repeated passes.

Keywords: UFG, SPD, DRECE.

1. Introduction

Severe Plastic Deformation (SPD) is a processing method used to produce ultrafine grained (UFG) materials by subjecting the material to extreme levels of hydrostatic pressure and shear deformation [1]. In general, fine-grained materials can exhibit excellent mechanical properties, such as high strength, high toughness, and superplasticity, even at room temperature [2, 3]. In fact, UFG materials are superior to coarse-grained materials in terms of mechanical properties and physical characteristics [4, 5]. SPD processes can be used to produce bulk materials with a UFG, which has great potential for the production of various industrial parts (finished or semi-finished products) [6–8].

However, the basic SPD processes: Equal-Channel Angular Pressing (ECAP) [9], High-Pressure Torsion (HPT) [10], and Accumulative Roll Bonding (ARB) [11], are limited for practical industrialisation because these discontinuous processes are difficult to apply in mass production [12]. To overcome such obstacles, continuous SPD processes have recently been invented using a variety of concepts by applying a continuous drag force to a workpiece [13]. Most of these are based on the ECAP process (e.g., constrain groove pressing [14], ECAP-Conform [15], equal channel angular rolling [16] and single roll angular rolling [17]). Continuous SPD forming technologies are widely used in manufacturing due to their minimal waste and low production costs, especially in the mass production of components. The choice of a suitable material depends on the requirements for the mechanical properties of the manufactured component, as well as the ability of the material to be plastically deformed without the ingress of local thinning or failure [18–21].

One of the most promising continuous SPD methods for processing of ferrous and non-ferrous metals and alloys is Dual Rolls Equal Channel Extrusion (DRECE) [22–24]. The DRECE method uses the principle of reproducible plastic forming to fragment the structure and improve the utility properties of the material. The material in sheet or strip form is fed into the forming zone by the main and auxiliary rolls and then pressed through the forming tool. The upper support and the upper die ensure the correct movement of the strip between the rollers during the process. The sheet metal strip is intensively deformed by a combination of bending and shearing as it passes through the deformation zone. The deformation causes gradual grain fragmentation due to the rearrangement of accumulated dislocations [25, 26].

The schematic illustration of the DRECE device is shown in Figure 1. The channel angle ϕ is one of the principal parameters of the DRECE process and has a significant effect on the material flow and the resulting microstructure. The channel angle ϕ,

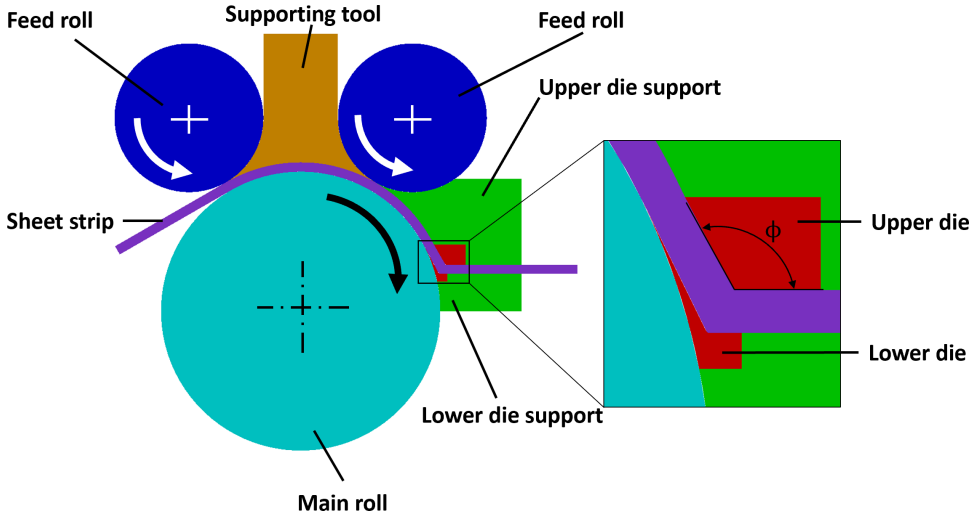

FIGURE 1. Schematic illustration of the Dual Rolls Equal Channel Extrusion (DRECE) process.

Element	Zn	Fe	Sn	C	Si	Pb	Al	Si	Cu
wt. %	37.064	0.048	0.029	0.026	0.022	0.016	0.003	0.003	Balan.

TABLE 1. Chemical composition CuZn37 alloy (obtained by optical emission spectroscopy).

namely the angle at which the inlet channel (between the upper die and the main roll) intersects with the outlet channel (between the lower and upper dies) plays a key role in the process efficiency.

2. Materials and methods

2.1. Experimental material

Commercial CuZn37 brass sheets, 2 mm thick, 58 mm wide, and 1 000 mm long, were subjected to the DRECE process at room temperature. The chemical composition of the alloy studied is given in Table 1. To homogenise the initial microstructure, the sheets were annealed at 450 °C for 1 h followed by air cooling.

2.2. Parameters of experiment

Prior to the DRECE process, both surfaces of the sheet were coated with MoS_2 lubricant to minimise friction. The rotation speed of the main roll was approximately 3 rpm, i.e. the linear speed of the DRECE processed strip is 10 mm s^{-1}. The pressure for the both feed rolls was 150 bar. The DRECE extrusion process was carried out with a channel angle of $\phi = 108°$. The DRECE process was carried out at room temperature and was repeated up to the fourth pass without rotation of the sheets between each pass. This is similar to the „Route A“ path in the conventional ECAP process [27].

Detailed studies of the microstructure in relation to the number of passes were carried out using optical microscopy (NIKON Epiphot 300) and transmission electron microscopy (Philips CM20 transmission electron microscope). The samples for the metallographic analysis were etched with $FeCl_3$+HCl+H_2O.

To evaluate the influence of the DRECE process on the mechanical properties of the CuZn37 alloy sheets, tensile and microhardness tests were carried out. For each pass, three specimens prepared along the extrusion direction, were used for tensile tests. The dimensions of the specimens for the tensile test were chosen according to ISO 6892-1 with an initial length of 55 mm. Tensile tests were carried out on the Zwick Z100 universal test machine at a strain rate of 1.0×10^{-3} s^{-1}. The Vickers microhardness was measured from the top to the lower surface of the sheets with a load of 100 g (HV0.1) and with a dwell time of 10 s. The samples were measured using LECO LM247AT microhardness tester. The evaluation of the tensile and microhardness measurement was carried out according to ISO 6892-1 and ISO 6507-4, respectively.

3. Results and discussion

3.1. Microstructure

Figure 2 shows the microstructure of the annealed brass prior to the DRECE process. The microstructure consists of α-brass grains with the occurance of annealing twins. The average grain size of the initial state was 70 µm (G4.7 according to ASTM E 112).

The microstructure of the samples after individual DRECE passes is shown in Figure 3. The microstructure of the samples after individual passes by the DRECE method is composed of α-brass with the occurrence of twins. After the plastic deformation, the appearance of slip lines and bands is evident. The frequency of slip lines and band occurrence increases with increasing number of passes (Figure 3a–3d). There is a slight elongation of the grains in the direction of the

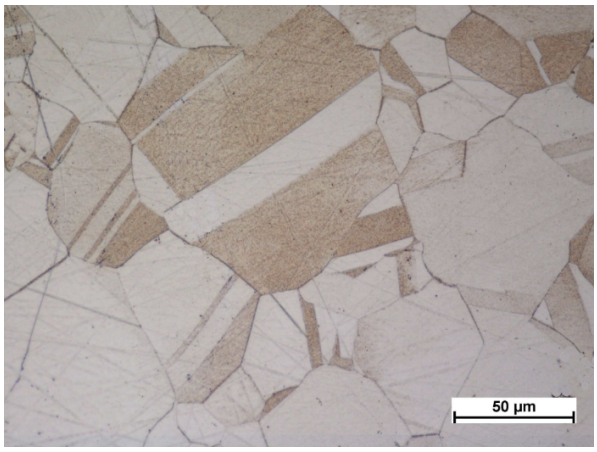

Figure 2. Microstructure of the initial state of the CuZn37 alloy.

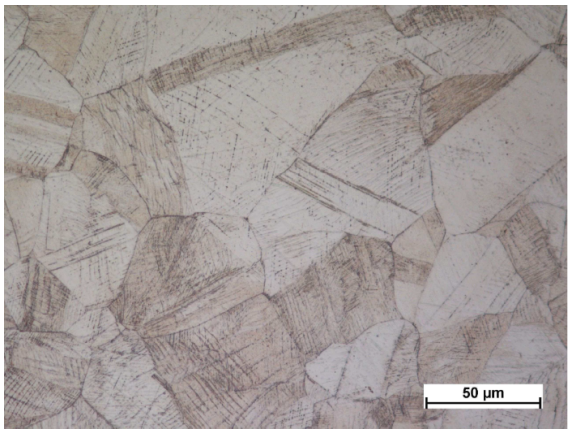

(a). First DRECE pass.

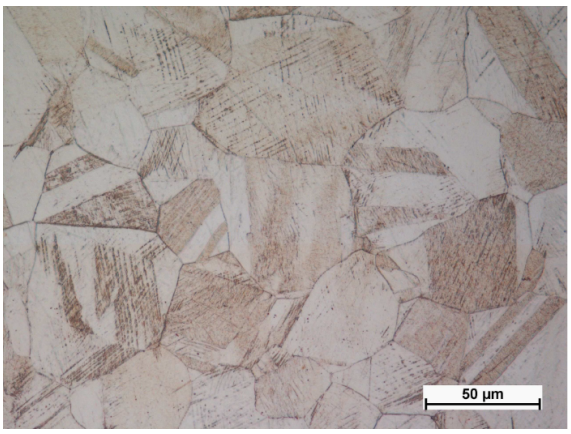

(b). Second DRECE pass.

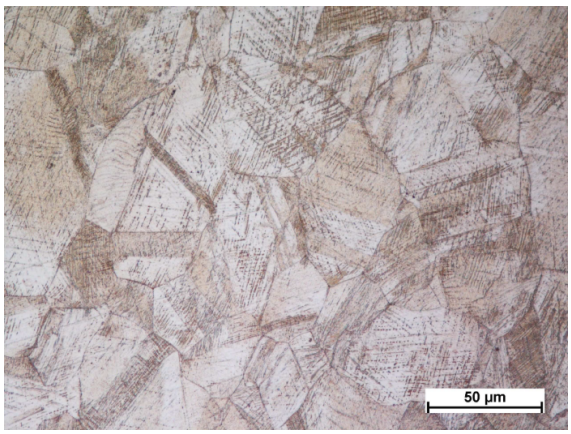

(c). Third DRECE pass.

(d). Fourth DRECE pass.

Figure 3. Microstructure of CuZn37 alloy processed by: first, second, third, and fourth DRECE passes.

DRECE extrusion with a higher intensity near the edges of the samples. The average grain size after each pass was relatively similar. After the first pass, the average grain size was 50 µm (G5.7). After subsequent passes, the average grain size was the same at 45 µm (G6.0).

Figure 4a shows the TEM micrograph of the sample that was passed once by the DRECE method. One can see that the grain refinement is not significant, only the growth of dislocation density and deformation twins can be observed. As indicated by the shape of the contour, no formation of subgrain boundaries can be seen. Additional DRECE processing, repeated four times, results in the formation of typical deformation twins and, in addition, the formation of a subgrain structure, which causes splitting of the diffraction spots in the direction of the diffraction pattern and produces a contrast typical of the orientation changes (Figure 4b). Similar to the first pass, a relatively high dislocation density can be seen.

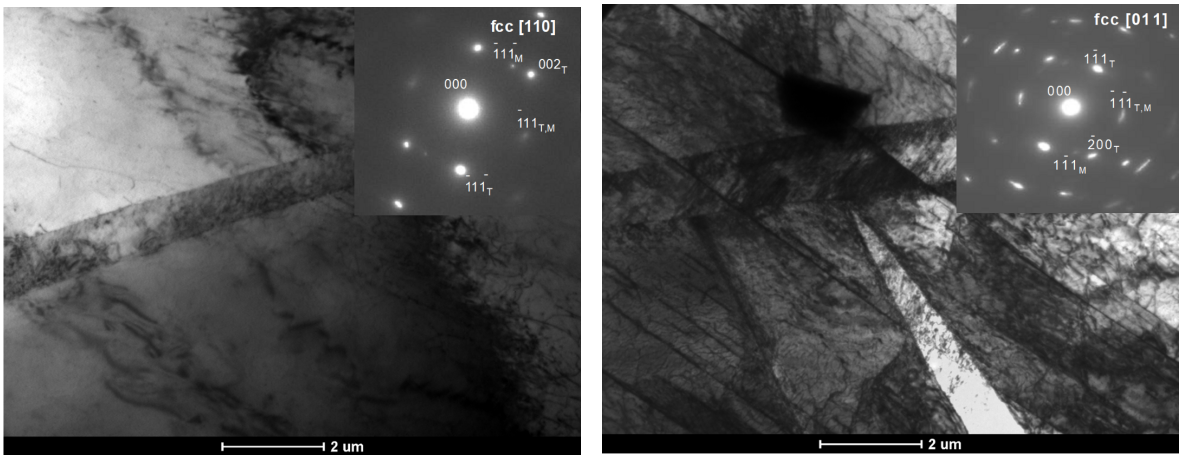

(A). First pass. (B). Fourth pass.

FIGURE 4. TEM micrographs of the DRECE processed CuZn37 alloy: after the first pass and after the fourth pass.

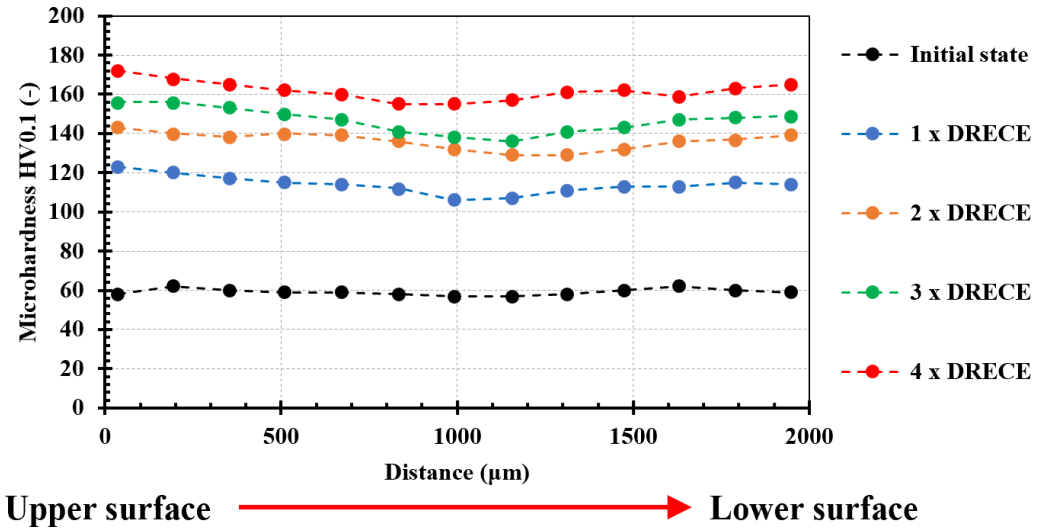

FIGURE 5. Vickers microhardness distributions from thetop to the bottom surface of the CuZn37 sheets processed by repeated DRECE passes.

3.2. MICROHARDNESS

Figure 5 shows the effect of the DRECE processing on the microhardness HV0.1 distribution in the thickness of the extruded CuZn37 sheets. It can be seen that the average microhardness increases with increasing number of passes. The extrusion of the sheet through the dies leads to an inhomogeneous distribution of the microhardness. Due to the combination of shear and flexural deformation that occurs during processing through dies, the microhardness decreases slightly towards the centre of the thickness. The decrease in microhardness between surfaces is typical for SPD processes based on the ECAP method [28]. Yoon showed that the distribution of microhardness inhomogeneity across the thickness of the severely deformed samples is fully dependent on the friction conditions and die geometry [29]. In the continuous SPD process for metal sheets, the deformation homogeneity induced by single pass is much more important than for metal bars because the metal sheets cannot be processed using the "Route BC", which is well known as a process route favourable to homogenising mechanical properties and microstructures during the ECAP process [30, 31].

As mentioned above, shear deformation alone cannot eliminate the less deformed zone in the middle of the sheet thickness. Therefore, it is necessary to take into account the inhomogeneous distribution of microhardness in the cross section of the DRECE processed sheets during the subsequent processing, as presented by Fang in [32].

3.3. TENSILE PROPERTIES

From the tensile stress-strain curves (Figure 6), it can be seen that the yield strength (σ_{YS}) and the ultimate tensile strength (σ_{UTS}) increased significantly after the first DRECE pass and reached the values of 262.3 MPa and 305.1 MPa, respectively. However, after each subsequent pass, the material was strengthened much less intensively than in the first pass. After the fourth pass, the highest values of σ_{YS} and σ_{UTS} for the tested material were obtained: 382.6 MPa and 420.8 MPa, respectively. In the initial state, the investigated alloy

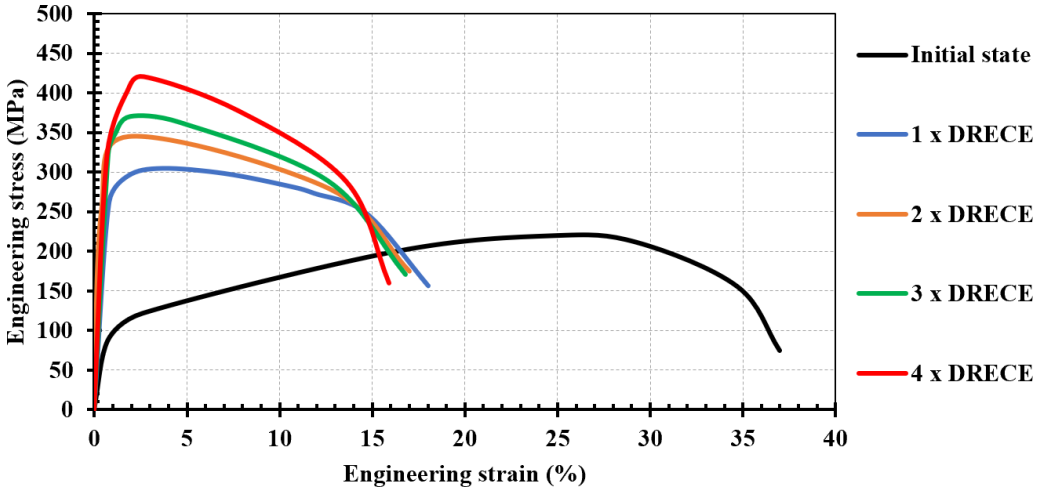

Figure 6. Tensile stress-strain curves of the CuZn37 alloy depending on the number of DRECE passes.

Sample	σ_{YS} [MPa]	σ_{UTS} [MPa]	At [%]
Initial state	96.5 ± 2.1	220.3 ± 1.9	37.1 ± 1.9
$1 \times$ DRECE	262.3 ± 5.2	305.1 ± 8.4	18.2 ± 1.3
$2 \times$ DRECE	305.3 ± 2.7	345.6 ± 1.3	17.1 ± 0.8
$3 \times$ DRECE	326.7 ± 0.8	370.9 ± 2.0	16.8 ± 1.4
$4 \times$ DRECE	382.6 ± 0.8	420.8 ± 1.1	15.9 ± 1.2

Table 2. Tensile properties depending on the number of DRECE passes.

exhibits very good plastic properties. However, as the number of passes increases, there is a significant decrease in the ductility. The total elongation (At) drops systematically from 37.1 % for the sample in the initial state to 15.9 % for the sample after the fourth pass. The average values of the standard tensile properties are summarised in Table 2.

During continuous SPD processes, the resulting tensile properties are predominantly affected by strain hardening and only minimally by the grain refinement effect. This phenomenon leads to a conventional trade-off tendency of strength-ductility, i.e. with an increasing number of passes, the tensile strength gradually increases and the ductility decreases [33]. In the case of grain refinement, there is no significant reduction in ductility due to the rearrangement and partial annihilation of the dislocation during the formation of subgrains [34].

4. Conclusion

In this study, the influence of the DRECE method on the microstructure and mechanical properties of commercial CuZn37 strips was systematically investigated. Based on the results obtained, the following conclusions were drawn:

- The microstructure consists of a single α-phase grains with low twin density. As the number of passes increased, there was an increased accumulation of dislocations, twins, and slip bands. The grain refinement of the investigated alloy was minimal (from the initial value of 70 µm to 45 µm after the fourth DRECE pass).
- TEM analysis confirmed the development of subgrains in the severely deformed microstructure after the fouth pass.
- The results of the microhardness distribution confirmed a inhomogeneous distribution of deformation in the cross-section of the sheet, which could be limited by the choice of a suitable deformation route.
- The tensile strength of the DRECE-processed brass strips increased with the number of passes. The most significant material strengthening was achieved after the first pass. In the following passes, the strengthening was less intensive. After the fourth pass, the yield strength of 382.6 MPa and the ultimate tensile strength of 420.8 MPa were achieved, which are significantly higher than the corresponding strength values characterising the material in the initial state (96.5 and 220.3 MPa, respectively). However, the elongation at break values decreased significantly with the number of passes. After four passes, it decreased to 15.9 % from 37.1 % in the initial state.
- All of the above knowledge could be applied in practice wherever it is necessary to achieve higher strength in CuZn37, e.g. tie rods, etc.

Acknowledgements

This article was supported by the Czech project No. SP2023/020 „Research and Optimisation of Engineer-

ing Technologies“ financed by the Ministry of Education, Youth and Sports of the Czech Republic. The publication was supported as a part of the project No. TH04010416 „Development of a new technology for refining steel strips“ financed by the Technology Agency of the Czech Republic.

References

[1] W. Maziarz, M. Greger, P. Długosz, et al. Effect of severe plastic deformation process on microstructure and mechanical properties ofAlSi/SiC composite. *Journal of Materials Research and Technology* **17**:948–960, 2022. https://doi.org/10.1016/j.jmrt.2022.01.023

[2] R. Čada, M. Štěpán. Solution of a suitable method of production of contactor forgings. *MM Science Journal* (March):6304–6313, 2023. https://doi.org/10.17973/MMSJ.2023_03_2022100

[3] K. Sternadelová, H. Krupová, D. Matýsek, P. Mohyla. Quality assessment of the vitreous enamel coating applied to the weld joint. *MM Science Journal* (March):6333–6338, 2023. https://doi.org/10.17973/MMSJ.2023_03_2022105

[4] Y. Shi, Y. Wang, W. Shang, et al. Influence of grain size distribution on mechanical properties and HDI strengthening and work-hardening of gradient-structured materials. *Materials Science and Engineering: A* **811**:141053, 2021. https://doi.org/10.1016/j.msea.2021.141053

[5] J. Dutkiewicz, S. Rusz, W. Maziarz, et al. Modification of microstructure and properties of extruded Mg-Li-Al alloys of α and $\alpha + \beta$ phase composition using ECAP processing. *Acta Physica Polonica A* **131**(5):1303–1306, 2017. https://doi.org/10.12693/APhysPolA.131.1303

[6] V. Schindlerová, I. Šajdlerová. Use of the dynamic simulation to reduce handling complexity in the manufacturing process. *Advances in Science and Technology Research Journal* **14**(1):81–88, 2020. https://doi.org/10.12913/22998624/113616

[7] R. Thilagavathi, J. Viswanath, L. Čepová, V. Schindlerová. Effect of inflation and permitted three-slot payment on two-warehouse inventory system with stock-dependent demand and partial backlogging. *Mathematics* **10**(21):3943, 2022. https://doi.org/10.3390/math10213943

[8] M. Bučko, V. Schindlerová, H. Krupová. Application of lean manufacturing methods in the production of ultrasonic sensor. *Tehnički vjesnik* **29**(5):1671–1677, 2022. https://doi.org/10.17559/TV-20220421141917

[9] O. Hilšer, S. Rusz, W. Maziarz, et al. Structure and properties of AZ31 magnesium alloy after combination of hot extrusion and ECAP. *Acta Metallurgica Slovaca* **23**(3):222–228, 2017. https://doi.org/10.12776/ams.v23i3.971

[10] L. V. Wilches Pena, L. Wang, B. G. Mellor, et al. Characterisation of white etching structures formed in annealed AISI 52100 through high pressure torsion (HPT). *Tribology International* **184**:108432, 2023. https://doi.org/10.1016/j.triboint.2023.108432

[11] H. Parvin, M. Kazeminezhad. Strength evolution during accumulative roll bonding of the metal matrix composite. *Journal of Materials Research and Technology* **24**:1513–1523, 2023. https://doi.org/10.1016/j.jmrt.2023.03.082

[12] R. Čada, P. Lošák. Optimization of bellows and tubes cutting by disc knife to achieve the minimum burr size. *MM Science Journal* (December):5373–5380, 2021. https://doi.org/10.17973/MMSJ.2021_12_2021104

[13] K. Kowalczyk, M. B. Jabłońska, M. Tkocz, et al. Effect of the number of passes on grain refinement, texture and properties of DC01 steel strip processed by the novel hybrid SPD method. *Archives of Civil and Mechanical Engineering* **22**(3):115, 2022. https://doi.org/10.1007/s43452-022-00432-6

[14] A. Shahmirzaloo, S. M. Hosseini, A. Siahsarani, et al. Influences of the constrained groove pressing on microstructural, mechanical, and fracture properties of brass sheets. *Materials Research Express* **7**(11):116526, 2020. https://doi.org/10.1088/2053-1591/abc9f2

[15] S. Atefi, M. H. Parsa, D. Ahmadkhaniha, et al. A study on microstructure development and mechanical properties of pure copper subjected to severe plastic deformation by the ECAP-Conform process. *Journal of Materials Research and Technology* **21**:1614–1629, 2022. https://doi.org/10.1016/j.jmrt.2022.09.103

[16] T. Kvačkaj, A. Kováčová, R. Kočisko, et al. Microstructure evolution and mechanical performance of copper processed by equal channel angular rolling. *Materials Characterization* **134**:246–252, 2017. https://doi.org/10.1016/j.matchar.2017.10.030

[17] H. H. Lee, J. I. Yoon, H. S. Kim. Single-roll angular-rolling: A new continuous severe plastic deformation process for metal sheets. *Scripta Materialia* **146**:204–207, 2018. https://doi.org/10.1016/j.scriptamat.2017.11.043

[18] K. Żaba, S. Puchlerska, Ł. Kuczek, et al. Effect of step size on the formability of Al/Cu bimetallic sheets in single point incremental sheet forming. *Materials* **16**(1):367, 2023. https://doi.org/10.3390/ma16010367

[19] O. Hilšer, S. Rusz, M. Pastrňák, R. Zabystrzan. Tensile properties and miicrohardness evolution in medium carbon sheets subjected to continuous SPD process. In *29th International Conference on Metallurgy and Materials (METAL 2020)*, pp. 339–343. 2020. https://doi.org/10.37904/metal.2020.3490

[20] E. Evin, M. Tomáš. Comparison of deformation properties of steel sheets for car body parts. *Procedia Engineering* **48**:115–122, 2012. Modelling of Mechanical and Mechatronics Systems. https://doi.org/10.1016/j.proeng.2012.09.493

[21] P. Petroušek, R. Kočiško, T. Kvačkaj, et al. Formability evaluation of aluminium alloys by FLD diagrams. *Acta Physica Polonica A* **131**(5):1344–1346, 2017. https://doi.org/10.12693/APhysPolA.131.1344

[22] S. Rusz, O. Hilšer, V. Ochodek, et al. Effect of severe plastic deformation on mechanical and fatigue behaviour of medium-c sheet steel. *Journal of Mining and Metallurgy, Section B: Metallurgy* **56**(2):161–170, 2020. https://doi.org/10.2298/JMMB190910008R

[23] M. B. Jabłońska, K. Kowalczyk, M. Tkocz, et al. Dual rolls equal channel extrusion as unconventional spd process of the ultralow-carbon steel: finite element simulation, experimental investigations and microstructural analysis. *Archives of Civil and Mechanical Engineering* **21**(1):25, 2021. https://doi.org/10.1007/s43452-020-00166-3

[24] S. Rusz, O. Hilšer, V. Ochodek, et al. Influence of SPD process on low-carbon steel mechanical properties. *MM Science Journal* (June):2910–2914, 2019. https://doi.org/10.17973/MMSJ.2019_06_201890

[25] M. Tkocz, K. Kowalczyk, T. Bulzak, et al. Finite element analysis of material deformation behaviour during DRECE: The sheet metal SPD process. *Archives of Civil and Mechanical Engineering* **23**(3):145, 2023. https://doi.org/10.1007/s43452-023-00671-1

[26] M. Koralnik, A. Dobkowska, B. Adamczyk-Cieślak, J. Mizera. The influence of the microstructural evolution on the corrosion resistance of cold drawn copper single crystals in NaCl. *Archives of Metallurgy and Materials* **65**(1):55–64, 2020. https://doi.org/10.24425/amm.2019.131096

[27] H. H. Lee, K. J. Hwang, H. K. Park, H. S. Kim. Effect of processing route on microstructure and mechanical properties in single-roll angular-rolling. *Materials* **13**(11):2471, 2020. https://doi.org/10.3390/ma13112471

[28] P. C. Yadav, N. K. Sharma, S. Sahu, S. Shekhar. Influence of short heat-treatment on microstructural and mechanical inhomogeneity of constrained groove pressed Cu-Zn alloy. *Materials Chemistry and Physics* **238**:121912, 2019. https://doi.org/10.1016/j.matchemphys.2019.121912

[29] S. C. Yoon, P. Quang, S. I. Hong, H. S. Kim. Die design for homogeneous plastic deformation during equal channel angular pressing. *Journal of Materials Processing Technology* **187–188**:46–50, 2007. https://doi.org/10.1016/j.jmatprotec.2006.11.117

[30] O. Hilšer, M. Pastrňák, S. Rusz. Finite element analysis of twist channel angular pressing. *MM Science Journal* (March):6314–6318, 2023. https://doi.org/10.17973/MMSJ.2023_03_2022101

[31] H. H. Lee, H. K. Park, J. Jung, et al. Multi-layered gradient structure manufactured by single-roll angular-rolling and ultrasonic nanocrystalline surface modification. *Scripta Materialia* **186**:52–56, 2020. https://doi.org/10.1016/j.scriptamat.2020.03.051

[32] X. T. Fang, G. Z. He, C. Zheng, et al. Effect of heterostructure and hetero-deformation induced hardening on the strength and ductility of brass. *Acta Materialia* **186**:644–655, 2020. https://doi.org/10.1016/j.actamat.2020.01.037

[33] S. E. Mousavi, A. Sonboli, M. Meratian, et al. Achieving an exceptional ductility at room temperature in a low SFE copper alloy fabricated by severe plastic deformation. *Materials Science and Engineering: A* **802**:140654, 2021. https://doi.org/10.1016/j.msea.2020.140654

[34] M. Ebrahimi, S. Attarilar, F. Djavanroodi, et al. Wear properties of brass samples subjected to constrained groove pressing process. *Materials & Design* **63**:531–537, 2014. https://doi.org/10.1016/j.matdes.2014.06.043